Joint Association, Trajectory, Offloading, and Resource Optimization in Air and Ground Cooperative MEC Systems

Chen Wang, Daosen Zhai, *Member, IEEE*, Ruonan Zhang, *Member, IEEE*, Lin Cai, *Fellow, IEEE*, Lei Liu, *Member, IEEE*, and Mianxiong Dong, *Member, IEEE*

***Abstract*—The air and ground cooperative mobile edge computing (MEC) network provides a new paradigm for the development of the Internet of Things (IoT), which enhances the coverage of the terrestrial base station (TBS) and deploys computing resources near IoT devices. In this paper, we construct a UAV-assisted MEC system for IoT networks and design a data processing procedure. The UAV collects data from devices as a relay and makes decisions to offload some tasks to the central server connected with the TBS, while the onboard edge server in the UAV can perform local computing. Furthermore, we jointly optimize the device association, UAV's trajectories, task offloading, and resource allocation to reduce the energy consumption of the entire system. To solve this problem, we decompose it into three tractable sub-problems and use the block coordinate descent (BCD) method to iteratively optimize each set of control variables. Among them, device association is formulated as a linear programming problem, while UAV's trajectory optimization is transformed into a convex problem by introducing slack variables and using successive convex approximation (SCA). The offloading and resource assignment problem is proved to be convex via theoretical analysis and problem transformation. In addition, we derive the optimal relationship between computation duration and computing energy, which greatly reduces the complexity of problems. Simulation results show that the designed system and the algorithms can significantly reduce the total energy consumption, and the offloading strategies have a decisive impact on computation energy consumption.**

***Index Terms*—IoT, MEC, UAV, energy consumption, joint optimization.**

Manuscript received 15 June 2023; revised 22 October 2023 and 25 February 2024; accepted 3 April 2024. Date of publication 16 April 2024; date of current version 19 September 2024. This work was supported in part by the National Natural Science Foundation of China under Grant 62232013, Grant 62271402, Grant 62171385 and Grant 62301447, in part by the open research fund of National Mobile Communications Research Laboratory, Southeast University under Grant 2023D06, in part by the Key Research and Development Plan of Shaanxi Province under Grant 2023-YBGY-250, Grant 2022ZDLGY05-07 and Grant 2023-ZDLGY-06, in part by Guangdong Basic and Applied Basic Research Foundation under Grant 2024A1515011533, in part by the Natural Science Foundation of Sichuan Province under Grant 2023NSFSC1377, and in part by the Innovation Foundation for Doctor Dissertation of Northwestern Polytechnical University under Grant CX2023060. The review of this article was coordinated by Prof. Xu Chen. *(Corresponding author: Daosen Zhai.)*

Chen Wang is with the School of Electronics and Information, Northwestern Polytechnical University, Xi'an 710072, China, and also with the Research and Development Institute, Northwestern Polytechnical University Shenzhen, Shenzhen 518063, China (e-mail: chen-@mail.nwpu.edu.cn).

Daosen Zhai is with Research and Development Institute, Northwestern Polytechnical University Shenzhen, Shenzhen 518063, China, also with the National Mobile Communications Research Laboratory, Southeast University, Nanjing 211189, China, and also with the School of Electronics and Information, Northwestern Polytechnical University, Xi'an 710072, China (e-mail: zhaidaosen@nwpu.edu.cn).

Ruonan Zhang is with the School of Electronics and Information, Northwestern Polytechnical University, Xi'an 710072, China (e-mail: rzhang@nwpu.edu.cn).

Lin Cai is with the Department of Electrical and Computer Engineering, University of Victoria, Victoria, BC V8P 5C2, Canada (e-mail: cai@ece.uvic.ca).

Lei Liu is with the State Key Laboratory of Integrated Service Networks, Xidian University, Xi'an 710071, China, and also with the Xidian Guangzhou Institute of Technology, Guangzhou 510555, China (e-mail: tianjiaoliulei@163.com).

Mianxiong Dong is with the Department of Sciences and Informatics, Muroran Institute of Technology, Muroran 050-8585, Japan (e-mail: mx.dong@csse.muroran-it.ac.jp).

Digital Object Identifier 10.1109/TVT.2024.3388512

I. Introduction

In RECENT years, with the advent of low-latency and high-reliability mobile communication networks and the emergence of new information technologies such as artificial intelligence (AI), Big Data, and cybersecurity, the Internet of Things (IoT) has ushered in new developments and opportunities [1]. Cutting-edge applications such as smart healthcare, smart home, autonomous driving, wearable devices, virtual reality (VR), and digital twin are gradually connecting people, machines, and things together [2], [3]. It is estimated that by 2025, the global number of IoT devices will exceed 30 billion [4]. However, complex data processing and heavy workloads bring high energy demands to the IoT, and the limited computing ability and energy reserve of IoT devices make it difficult to perform complex computing tasks [5], [6]. Besides, uploading tasks to central servers can cause severe network congestion and instability.

A. Motivation

Regarding the aforementioned issues, mobile edge computing (MEC) is deemed a viable solution. The most important feature of MEC is its capability to deploy computing resources in close proximity to users [7], such that computation offloading can be implemented. Computation offloading transfers tasks from user devices to servers, which helps conserve the battery life of IoT devices [7]. Furthermore, edge servers are much closer to IoT devices than central servers, significantly reducing the transmission power consumption of IoT devices and base stations [8].

Thus, MEC effectively bridges the gap between IoT devices and centralized clouds [9], while also striking the optimal balance between local computing and offloading consumption [10].

However, there are still some drawbacks in traditional ground-based MEC networks. Specifically, IoT devices are mostly located in complex environments where it is often difficult to obtain good coverage from base stations, and they consume a lot of energy to communicate with the base station or offload tasks to edge servers. As a potential solution, unmanned aerial vehicles (UAVs) with deployability and flexibility [11] can serve as access points [12], [13] to relay the data between IoT devices and base stations, shorten the communication distance, and facilitate the establishment of line-of-sight (LOS) channels [14], [15]. In addition, UAVs can carry edge servers and dynamically deploy them near devices, thereby reducing the energy consumption required for task offloading. Moreover, the nearby edge servers ensure low processing latency for device tasks.

Integrating UAVs with MEC introduces new factors to consider while improving network performance, including: (1) the impact of UAVs deployment on network architecture, (2) the interaction process between devices and UAVs, (3) collaboration between UAVs and ground stations, especially regarding task offloading and resource allocation. In current research, while there have been many studies exploring the integration of MEC networks with UAVs, most of these studies have primarily focused on the aerial network, with limited attention given to the collaborative computing between UAVs and ground base stations. Furthermore, there is relatively limited research that comprehensively considers the impact of network parameters on the data processing workflow. Most existing work predominantly focuses on task offloading while overlooking the global optimization of the network.

Therefore, in this paper, we consider the collaboration between the UAV and ground-based station when designing the network architecture. Specifically, we utilize the UAV as an aerial access point to collect data and simultaneously as an edge server to assist the base station in computing. Additionally, we construct a comprehensive data processing model, divide time slots on the time scale, and design the data processing mechanism. Moreover, we simultaneously consider the IoT devices association, UAV's trajectory, task offloading, and resource allocation to reduce the total energy expenditure of the whole system.

B. Contributions

The main contributions are summarized as follows.

- *We design a MEC system assisted by UAV in IoT networks:* The UAV collects data from IoT devices, makes decisions on task offloading during dynamic flight, and acts as an edge server to assist the central server connected to the TBS in the data processing.
- *We devise a comprehensive data processing flow:* On the time scale, we divide the task completion time into slots and schedule the association of IoT devices to ensure task completion. At the same time, we design three stages in each time slot to optimize the data processing procedure.
- *We propose the JATOR algorithm to minimize the overall energy consumption of the system:* Considering network-wide energy consumption, we jointly optimize device association, trajectory, offloading, and resource allocation. We decompose this into three tractable sub-problems solved iteratively with BCD. Device association becomes a linear programming problem, UAV trajectory optimization turns convex with slack variables and SCA. Task offloading and resource allocation are fully decoupled and proven to be convex for obtaining approximate optimal solutions.
- *Simulations demonstrate that our algorithms can significantly reduce the total energy consumption:* Simulation results also confirm our proposition that the effective capacitance of server, amount of data, and communication rate affect the optimal offloading ratio, which in turn decisively impacts computation energy consumption.

C. Organization

We structure this paper in the following manner. In Section II, we provide an overview of related works. Section III introduces the designed UAV-assisted MEC system, and the joint device association, trajectory planing, task offloading, and resource allocation problem. We decompose this problem into three sub-problems and propose the JATOR algorithm in Section IV. In Section V, we present the simulation results and analysis, which demonstrate the performance of our proposed system and algorithms. Finally, we summarize the paper in Section VI.

II. Related Works

In this section, we introduce the related works on energy-saving aspects of MEC [16], [17], [18], [19], [20], [21], [22], [23] and UAV-assisted MEC [24], [25], [26], [27], [28], [29], [30], [31], [32].

A. MEC

In [16], the authors studied offloading strategies combined with non-orthogonal multiple access (NOMA) techniques in MEC networks with multiple users and proposed an optimization problem for minimizing energy consumption. In [17], the authors focused on maximizing energy efficiency by synthetically considering the computation amount and energy expenditure. They derived closed-form solutions for partial offloading in a designed NOMA-based MEC network. Task offloading schemes coupled with energy harvesting (EH) were investigated in the MEC system in [18] to minimize long-term average energy consumption of all devices. The authors in [19] designed the MEC system and frame structure for EH and task processing and formulated an optimization problem considering resource allocation and computation offloading to maximize energy efficiency. In [20], the authors proposed a long-term average energy-efficient optimization problem in the MEC system with stochastic network states and investigated the trade-off between energy efficiency and latency. In [21], a joint communication and resource allocation problem was formulated to maximize energy efficiency in the NOMA-based MEC network, while

considering multiple cells and complicated interference. To minimize the weighted sum energy of all devices and MEC server, the authors in [22] proposed a joint transmission, computation, and wireless charging optimization problem subject to latency and power constraints. In [23], a joint offloading and balancing optimization problem in the MEC system was investigated to reduce long-term weighted sum energy and latency expenditure.

B. UAV-Assisted MEC

In [24], a dynamic UAV was employed instead of a base station to provide edge computing services, and the authors formulated a stochastic optimization problem to minimize the weighted energy consumption of all devices. Similarly, in [25], a UAV carrying a computing server was deployed in the MEC system, and resource allocation and UAV trajectory were jointly optimized in OMA and NOMA modes to reduce weighted energy consumption. In [26], the authors focused on improving the energy efficiency of UAVs by studying UAV trajectory and resource allocation in the MEC system. Multiple UAVs were deployed in the MEC network in [27] to provide edge computing for devices, and the authors proposed a decoupled weighted energy consumption minimization problem. The problem of minimizing UAV energy consumption in the MEC system was formulated as a stochastic programming problem in [28], which involved data queue stability and was solved using Lyapunov optimization. In [29], the authors deployed a UAV above IoT devices as a server with predetermined initial and final locations, and optimized the trajectory, offloading, and resource allocation to reduce the UAV's energy consumption and completion time. In [30], a UAV was utilized to provide computing and communication services for mobile vehicular users in the MEC network, and the weighted sum energy efficiency of the entire system was optimized. The authors in [31] introduced an access point in the MEC network, enabling the UAV to offload tasks further. In [32], the UAV was considered as an energy transmitter and edge server providing power and services. The authors in [33] proposed a task scheduling policy aimed at minimizing both computing and offloading delays for all tasks, considering the constraint of UAV energy capacity.

III. System Model and Problem Formulation

As shown in Fig. 1, we devise an air-and-ground collaborative MEC system for IoT networks, which includes K IoT devices distributed in complex environments denoted as $\mathcal{K}$, a TBS linked with the central server for remote computing, and a rotatory wing UAV equipped with edge server to provide local computing service. The UAV and IoT devices constitute the terrestrial access network, and the aerial relay network includes the TBS and the UAV.

A. Communication Model

In the system, IoT devices generate raw data periodically, e.g., surveillance video, orientation information, environment monitoring data and so on. We assume that each IoT device generates L bits data in periodic time T. Due to the complex

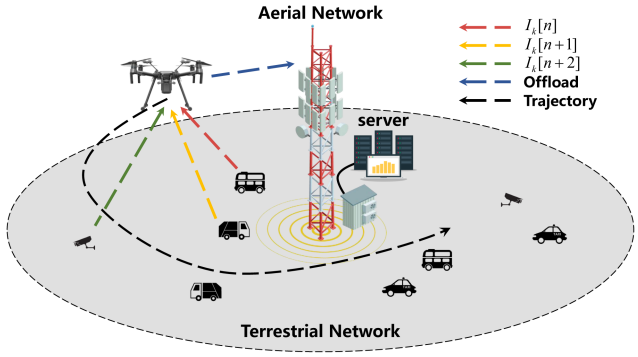

Fig. 1. UAV-assisted MEC network.

environments of IoT devices and their weak computing ability, a UAV is deployed to hover above them to establish communication links and collect data for further processing. Taking the position of the TBS as the origin, we represent the horizontal coordinates of the TBS and k-th IoT device as $\mathbf{w}_t = (0, 0)$ and $\mathbf{w}_k = (x_k, y_k)$, respectively. Besides, we assume that the altitude of the TBS and the UAV is a constant value H for simplicity. It is difficult to describe the location of the UAV because it is constantly in motion. For simplicity, we discrete the time period T into multiple uniform time slots denoted as $\mathcal{N} = \{1, 2, ..., N\}$ with each slot length $t = T/N$. Considering the time slot length and UAV's maximal speed, the location of the UAV in each time slot can be roughly regarded as fixed [34]. Therefore, we can denote the location of the UAV in the n-th time slot as $\mathbf{w}_u[n] = (x_u[n], y_u[n])$. In the system, the UAV hovers above the IoT devices and the trajectory is restricted by the following initial location[1] and maximal speed constraints

$$\mathbf{w}_u\left[1\right] = \mathbf{w}_u\left[N\right], \tag{1}$$

$$\left\|\mathbf{w}_u\left[n+1\right] - \mathbf{w}_u\left[n\right]\right\| \leq V_{\max} t,\ n = 1, \ldots, N-1, \tag{2}$$

where $V_{\max}$ denotes the maximal speed of the UAV. And the flying energy of the UAV is related to speed [35], we describe it as

$$E_{fly}\left[n\right] = \kappa \|\mathbf{w}_u\left[n+1\right] - \mathbf{w}_u\left[n\right]\|^2, n = 1, \ldots, N-1, \tag{3}$$

where constant κ represents a weighting factor.

According to the coordinates of the UAV and IoT devices, we can indicate the distance between IoT device k and the UAV in the n-th time slot with $d_k[n] = \sqrt{H^2 + \|\mathbf{w}_u[n] - \mathbf{w}_k\|^2}$. For the channel model between the UAV and IoT devices, we adopt the large-scale fading model, in which the channel quality is determined by distance and the Doppler effect can be ignored considering the UAV's speed [34]. Thus, the channel power gain from IoT device k to the UAV in time slot n can be written as

$$h_k\left[n\right] = \rho_0 d_k^{-2}\left[n\right] = \frac{\rho_0}{H^2 + \left\|\mathbf{w}_u\left[n\right] - \mathbf{w}_k\right\|^2}, \tag{4}$$

[1]It is noteworthy that we specify the UAV's landing position to be the same as its initial position. This allows the UAV to promptly replace the battery upon completing its flight task. Moreover, in the optimization problem, the energy consumption of the UAV is also incorporated as part of the objective function. These collectively tackle the challenge of limited energy for UAV.

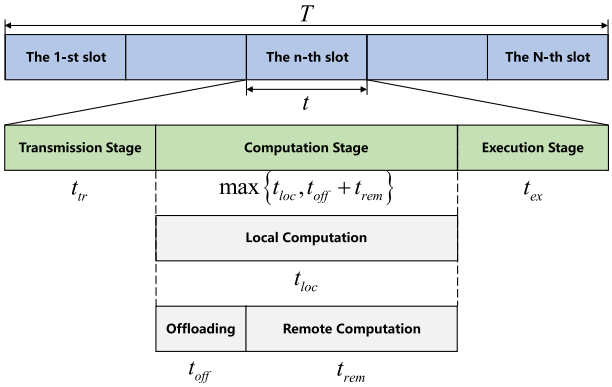

Fig. 2. Data processing procedure.

where ρ_0 represents the reference channel power gain with distance $d_{ref} = 1\ m$ [34]. Furthermore, we specify that only one IoT device can transmit data to the UAV at the same time, and the frequency of the terrestrial network differs from that of the aerial network, so the data transmission will not be interfered. Denote the bandwidth of terrestrial network with B and the transmitting power of IoT device k with P_k respectively, we can describe the transmission rate of device k in time slot n as

$$R_k[n] = B\log_2\left(1 + \frac{P_k h_k[n]}{\sigma^2}\right), \tag{5}$$

where σ^2 refers to the noise power.

For the link in the aerial network, since there is a line-of-sight (LOS) channel between the UAV and the TBS, and the TBS can enhance the communication through advanced technologies such as beamforming, high-power transmitter, adaptive modulation and coding, etc., so the transmission rate from the UAV to the TBS can reach a satisfying value. And in this paper, the communication rate of the aerial network has little effect on the problem, so we regard the transmission rate from the UAV to the TBS as a reasonable constant R_u.

B. Data Processing Model

The data processing in each time slot is shown in Fig. 2, which includes three stages: transmission, computation, and execution. In the transmission stage, the UAV hovers above the IoT devices to collect their data for further complicated analysis and processing. After aggregating the raw data, the UAV makes offloading strategies to process a part of data locally and offloads the remaining to the TBS for computing. Finally, the results are transmitted separately to each IoT device for subsequent executions.

1) Transmission Stage: We specify the t_{tr} time length at the beginning of each time slot as the transmission stage, which is used for IoT devices to transmit data to the UAV in the time division multiple access (TDMA) manner. We define a continuous association control variable $0 \le I_k[n] \le 1$, which presents that the k-th IoT device occupies a transmission time with the proportion of $I_k[n]$ to access the UAV in the n-th time slot. Furthermore, there exists the association upper limit constraint $\sum_{k=1}^{K} I_k[n] \le 1,\ \forall n$. Therefore, the aggregated data from IoT devices in the n-th time slot can be denoted as

$$L[n] = \sum_{k=1}^{K} I_k[n] R_k[n] t_{tr}. \tag{6}$$

And the energy consumption in the transmission stage can be written as

$$E_{tr}[n] = \sum_{k=1}^{K} I_k[n] P_k t_{tr}. \tag{7}$$

2) Computation Stage: After collecting the raw data from IoT devices, data processing enters the computation stage, which includes the local computation at the UAV and the remote computation at the central server. We assume that data can be independently computed in bits and that data segmentation can be viewed as continuous compared to the total data size [36]. We define that the UAV offloads the raw data of the $0 \le r[n] \le 1$ ratio to the TBS, and part of the $(1 - r[n])$ raw data is processed locally at the UAV in the n-th time slot. We further stipulate that the CPU frequency required to compute a bit of data is C (cycles per bit), and the edge server adopts the dynamic frequency scaling (DFS) technology, which means that the computing energy consumption can be optimized by adjusting the allocated CPU frequency. Denote the allocated edge server CPU frequencies in the n-th time slot as $f_u[n]$ (cycles per second). Then the local computation time can be formulated as

$$t_{loc}[n] = \frac{(1 - r[n]) L[n] C}{f_u[n]}, \tag{8}$$

which is constrained by the length of time slot, as described later. And the local computation energy [36] can be formulated as

$$E_{loc}[n] = \psi f_u^3[n] t_{loc}[n], \tag{9}$$

where ψ is an effective capacitance coefficient [37].

At the same time as the local computation, the UAV offloads the $r[n]$ ratio of data to the TBS for remote computation. Thus, we can calculate the offloading time according to R_u as

$$t_{off}[n] = \frac{r[n] L[n]}{R_u}, \tag{10}$$

and the energy consumption can be indicated as

$$E_{off}[n] = P_u t_{off}[n], \tag{11}$$

where P_u represents the total required power of the UAV to offload data. After the data offloading is completed, the time required for remote computation at the central server $t_{rem}[n]$ can be formulated as

$$t_{rem}[n] = \frac{r[n] L[n] C}{f_s[n]}, \tag{12}$$

where $f_s[n]$ denotes the allocated CPU frequencies of the central server in the n-th time slot. And the remote computation energy [36] can be formulated as

$$E_{rem}[n] = \varphi f_s^3[n] t_{rem}[n], \tag{13}$$

where φ denotes the effective capacitance coefficient of the central server.

It should be noted that, as shown in Fig. 2, local computation can be executed in parallel with offloading and remote computation, with the duration of the computation stage being the larger of the two, i.e., $\max\{t_{loc}[n], t_{off}[n] + t_{rem}[n]\}$.

3) Execution Stage: After the computation stage is completed, the instructions to be executed are sent out by the UAV and the TBS to IoT devices respectively, which only have few bits compared to the raw data. Thus, the consumed time is very short and can be regarded as a fixed value t_{ex}.

We specify that the total time of the above three stages should not exceed the time slot length, i.e.,

$$t_{tr} + \max\left\{t_{loc}\left[n\right], t_{off}\left[n\right] + t_{rem}\left[n\right]\right\} + t_{ex} \leq t. \tag{14}$$

And we denote the total energy of the above three stages in a period as

$$E = \sum_{n=1}^{N} \left(E_{tr}\left[n\right] + E_{loc}\left[n\right] + E_{off}\left[n\right] + E_{rem}\left[n\right]\right) + \sum_{n=1}^{N-1} E_{fly}\left[n\right]. \tag{15}$$

C. Problem Formulation

In this system, the device association and the UAVs' trajectory are the bases of data processing, which determine the transmitted data amount and communication rate in each time slot separately. Besides, the offloading strategies and CPU frequencies allocation have an great influence on the time and energy consumption of local and remote computation. To minimize the entire energy of the designed system, we jointly optimize the association control ($\mathbf{I}$), UAV's trajectory ($\mathbf{W}$), offloading strategies ($\mathbf{R}$), and CPU frequencies allocation ($\mathbf{F}_u$ and $\mathbf{F}_s$) in each time slot. Therefore, the joint optimization problem is formulated as

$$\min_{\mathbf{I},\mathbf{W},\mathbf{F},\mathbf{R}} E \tag{16}$$

$$\text{s.t. C1}: \ 0 \leq I_k\left[n\right] \leq 1, \ \forall k, n \tag{16a}$$

$$\text{C2}: \ \sum_{k=1}^{K} I_k\left[n\right] \leq 1, \ \forall n \tag{16b}$$

$$\text{C3}: \ \mathbf{w}_u\left[1\right] = \mathbf{w}_u\left[N\right] \tag{16c}$$

$$\text{C4}: \ \left\|\mathbf{w}_u\left[n+1\right] - \mathbf{w}_u\left[n\right]\right\| \leq V_{\max} t, \ n = 1, \ldots, N-1 \tag{16d}$$

$$\text{C5}: \ 0 \leq f_u\left[n\right] \leq F_u, \ \forall n \tag{16e}$$

$$\text{C6}: \ 0 \leq f_s\left[n\right] \leq F_s, \ \forall n \tag{16f}$$

$$\text{C7}: \ 0 \leq r\left[n\right] \leq 1, \ \forall n \tag{16g}$$

$$\text{C8}: \ t_{tr} + \max\left\{t_{loc}\left[n\right], t_{off}\left[n\right] + t_{rem}\left[n\right]\right\} + t_{ex} \leq t, \forall n \tag{16h}$$

$$\text{C9}: \ \sum_{n=1}^{N} I_k\left[n\right] R_k\left[n\right] t_{tr} \geq L, \ \forall k, \tag{16i}$$

TABLE I
NOTATIONS

Description of Specifications	Notation
Number of IoT devices	K
Amount of data generated by each IoT device	L
Length of the periodic time	T
Height of the TBS and UAV	H
Number of time slots	N
Length of time slots	t
Maximal speed of the UAV	V_{max}
Weighting factor of flying energy consumption	κ
Channel power gain at the distance d_{ref}	ρ_0
Bandwidth of IoT devices	B
Transmitting power of IoT devices	P_k
Noise power	σ^2
Transmission rate from the UAV to the TBS	R_u
Length of transmission stage	t_{tr}
Number of CPU cycles needed for one bit of data	C
Effective capacitance coefficient of the UAV	ψ
Required power of UAV to offload data	p_m
Effective capacitance coefficient of the TBS	φ
Length for execution stage	t_{ex}
Maximal CPU frequencies of the edge server	F_u
Maximal CPU frequencies of the central server	F_s

where F_u and F_S present the maximal CPU frequencies of the edge server and central server, respectively.

In (16), constraints C1 and C2 limit the association control of IoT devices. Constraints C3 and C4 denote initial location and maximal speed of the UAV. Constraints C5 and C6 restrict the allocated CPU frequencies of the edge and central servers separately. Constraint C7 denotes the offloading ratio restrict. Constraint C8 restricts the length of each time slot. And constrain C9 ensures that all the data from each IoT device can be processed in each period.

IV. Problem Transformation and Algorithm Design

The problem in (16) is challenging because it includes complex constraints and variables. Specifically, the objective function is to minimize the total energy consumption of three stages in every time slot, which contains contradictory terms in each time slot and between different time slots, e.g., local and remote computation energy. Besides, C8 and C9 are non-convex constraints involving all the variables. To solve this problem, we first deal with the constraint C8 and transform it into

$$t_{loc}[n] \leq t_{\max}, \ \forall n \tag{17}$$

and

$$t_{off}\left[n\right] + t_{rem}\left[n\right] \leq t_{\max}, \ \forall n \tag{18}$$

where $t_{\max} = t - t_{tr} - t_{ex}$ denotes the maximal time length of computation stage. By splitting Constraint C8 into two separate constraints, the problem is relieved from the challenge of dealing with a maximization function. And the problem can be rewritten as

$$\min_{\mathbf{I},\mathbf{W},\mathbf{F},\mathbf{R}} E \tag{19}$$

$$\text{s.t. C1}: \ \frac{\left(1 - r\left[n\right]\right) L\left[n\right] C}{f_u[n]} \leq t_{\max}, \ \forall n \tag{19a}$$

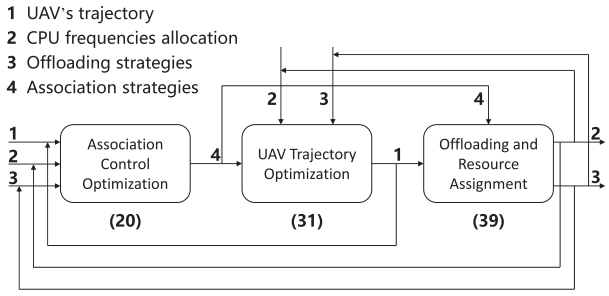

Fig. 3. Overall algorithm.

$$\text{C2}: \ \frac{r[n]L[n]}{R_u} + \frac{r[n]L[n]C}{f_s[n]} \le t_{\max}, \ \forall n \tag{19b}$$

$$\text{C3}: \ \text{(16a)–(16g), (16i).} \tag{19c}$$

In the problem, device association and UAV's trajectory have an earlier logical sequence than offloading and computing frequencies allocation. Besides, the UAV's trajectory is more independent than device association in the objective function and constraints. Thus, we divide problem (19) into three tractable sub-problems: device association optimization, UAV's trajectory optimization, and offloading and resource assignment, which are solved by the BCD method.

The main procedure of the overall algorithm is shown in Fig. 3. We first determine the UAV's trajectory, CPU frequency allocation, and task offloading strategies. Then, we solve the association control problem to obtain the device association strategies. Next, we utilize the updated device association and optimize the UAV's trajectory based on the initial CPU frequency allocation and task offloading strategies. Finally, we solve the offloading and resource allocation problem. In the following iterations, the initial variables are replaced with the updated values from the last iteration.

A. Association Control Optimization

We first give the UAV's trajectory ($\mathbf{W}$), CPU frequencies allocation ($\mathbf{F}_u$ and $\mathbf{F}_s$), and offloading strategies ($\mathbf{R}$) initial values $\mathbf{W}^0$, $\mathbf{F}_u^0$, $\mathbf{F}_s^0$, and $\mathbf{R}^0$ to optimize device association. The initial values should be set appropriately to satisfy the constraints (16c)–(16g). And based on the initial values, we can formulate the device association optimization problem as

$$\min_{\mathbf{I}} \ \sum_{n=1}^{N} \left(E_{tr}[n] + E_{loc}[n] + E_{off}[n] + E_{rem}[n]\right) \tag{20}$$

$$\text{s.t. C1}: \ 0 \le I_k[n] \le 1, \ \forall k, n \tag{20a}$$

$$\text{C2}: \ \sum_{k=1}^{K} I_k[n] \le 1, \ \forall n \tag{20b}$$

$$\text{C3}: \ \frac{(1-r[n])L[n]C}{f_u[n]} \le t_{\max}, \ \forall n \tag{20c}$$

$$\text{C4}: \ \frac{r[n]L[n]}{R_u} + \frac{r[n]L[n]C}{f_s[n]} \le t_{\max}, \ \forall n \tag{20d}$$

$$\text{C5}: \ \sum_{n=1}^{N} I_k[n] R_k[n] t_{tr} \ge L, \ \forall k, \tag{20e}$$

which only contains the variable $\mathbf{I}$ and the constraints are all linear (Notice that $L[n]$ in C3 and C4 is a linear function of $\mathbf{I}$). According to (7), $E_{tr}[n]$ in the objective function is linear with respect to $\mathbf{I}$. Furthermore, the rest part of the objective function can also be transformed as the following linear function of $\mathbf{I}$ by substituting formulas (9), (11), and (13).

$$\begin{aligned}
&\sum_{n=1}^{N} \left(E_{loc}[n] + E_{off}[n] + E_{rem}[n]\right) \\
&= \sum_{n=1}^{N} \left(\psi f_u^3[n] t_{loc}[n] + P_u t_{off}[n] + \varphi f_s^3[n] t_{rem}[n]\right) \\
&= \sum_{n=1}^{N} \Bigg(\psi f_u^2[n](1-r[n])L[n]C + \frac{P_u r[n] L[n]}{R_u} \\
&\quad + \varphi f_s^2[n] r[n] L[n] C\Bigg) \\
&= \sum_{n=1}^{N}\sum_{k=1}^{K} I_k[n] R_k[n] t_{tr} \Bigg(\psi f_u^2[n](1-r[n])C + \frac{P_u r[n]}{R_u} \\
&\quad + \varphi f_s^2[n] r[n] C\Bigg).
\end{aligned} \tag{21}$$

Thus, the device association problem (20) is a linear programming problem, and we adopt the mathematical solver Gurobi to find the optimal solution.

B. UAV's Trajectory Optimization

After acquiring association strategies of IoT devices by solving problem (20), we replace $\mathbf{I}^0$ with the result $\mathbf{I}$ as part of inputs to optimize the trajectory $\mathbf{W}$. The rest of the variables are still the initial values $\mathbf{F}_u^0$, $\mathbf{F}_s^0$, and $\mathbf{R}^0$. Then the UAV trajectory optimization problem can be formulated as

$$\min_{\mathbf{W}} \ \sum_{n=1}^{N-1} E_{fly}[n] \tag{22}$$

$$\text{s.t. C1}: \ \mathbf{w}_u[1] = \mathbf{w}_u[N] \tag{22a}$$

$$\text{C2}: \ \|\mathbf{w}_u[n+1] - \mathbf{w}_u[n]\| \le V_{\max} t, \ n = 1, \ldots, N-1 \tag{22b}$$

$$\text{C3}: \ \frac{(1-r[n])\sum_{k=1}^{K} I_k[n] R_k[n] t_{tr} C}{f_u[n]} \le t_{\max}, \ \forall n \tag{22c}$$

$$\text{C4}: \ \frac{r[n]\sum_{k=1}^{K} I_k[n] R_k[n] t_{tr}}{R_u} + \frac{r[n]\sum_{k=1}^{K} I_k[n] R_k[n] t_{tr} C}{f_s[n]} \le t_{\max}, \ \forall n \tag{22d}$$

$$\text{C5}: \sum_{n=1}^{N} I_k[n] R_k[n] t_{tr} \geq L, \forall k. \tag{22e}$$

According to the definition of E_{fly} in (3), the objective function is convex with respect to $\mathbf{W}$. Further, the constraint (22a) is linear and (22b) is a convex quadratic constraint. Since the constraints (22c)–(22e) have complex forms, we substitute $R_k[n]$ into them for the sake of analysis. Then (22c) and (22d) can be transformed into

$$\sum_{k=1}^{K} I_k[n] B\log_2\left(1+\frac{P_k\rho_0}{\sigma^2(H^2+\|\mathbf{w}_u[n]-\mathbf{w}_k\|^2)}\right) t_{tr} \leq \frac{(1-r[n]) f_u[n]}{C} t_{\max}, \forall n, \tag{23}$$

and

$$\sum_{k=1}^{K} I_k[n] B\log_2\left(1+\frac{P_k\rho_0}{\sigma^2(H^2+\|\mathbf{w}_u[n]-\mathbf{w}_k\|^2)}\right) t_{tr} \leq \frac{R_u f_s}{r[n](f_s+R_u C)} t_{\max}, \forall n. \tag{24}$$

For the transformation of (22e), it has a different direction than (22c) and (22d), and can be expressed as

$$\sum_{n=1}^{N} I_k[n] B\log_2\left(1+\frac{P_k\rho_0}{\sigma^2(H^2+\|\mathbf{w}_u[n]-\mathbf{w}_k\|^2)}\right) t_{tr} \geq L, \forall k. \tag{25}$$

We can find that constraints (23)–(25) are non-convex, which makes problem (22) hard to tackle by efficient methods. So we attempt to convert (23)–(25) to convex constraints.

We first deal with the non-convexity of constraints (23) and (24). Although $R_k[n]$ is neither convex nor concave with respect to $\mathbf{w}_u[n]$, (23) and (24) are convex with respect to $\|\mathbf{w}_u[n]-\mathbf{w}_k\|^2$. Thus, we can introduce slack variables $\mathbf{S}=\{S_k[n] \leq \|\mathbf{w}_u[n]-\mathbf{w}_k\|^2, \forall k,n\}$ to replace $\|\mathbf{w}_u[n]-\mathbf{w}_k\|^2$, and reformulate problem (22) as

$$\min_{\mathbf{W},\mathbf{S}} \sum_{n=1}^{N-1} E_{fly}[n] \tag{26}$$

$$\text{s.t. C1}: \mathbf{w}_u[1]=\mathbf{w}_u[N] \tag{26a}$$

$$\text{C2}: \|\mathbf{w}_u[n+1]-\mathbf{w}_u[n]\| \leq V_{\max} t,\ n=1,\ldots,N-1 \tag{26b}$$

$$\text{C3}: \sum_{k=1}^{K} I_k[n] B\log_2\left(1+\frac{P_k\rho_0}{\sigma^2(H^2+S_k[n])}\right) t_{tr} \leq \frac{(1-r[n]) f_u[n]}{C} t_{\max}, \forall n, \tag{26c}$$

$$\text{C4}: \sum_{k=1}^{K} I_k[n] B\log_2\left(1+\frac{P_k\rho_0}{\sigma^2(H^2+S_k[n])}\right) t_{tr} \leq \frac{R_u f_s}{r[n](f_s+R_u C)} t_{\max}, \forall n \tag{26d}$$

$$\text{C5}: S_k[n] \leq \|\mathbf{w}_u[n]-\mathbf{w}_k\|^2, \forall k,n \tag{26e}$$

$$\text{C6}: (25). \tag{26f}$$

Since $S_k[n]$ is always less than or equal to $\|\mathbf{w}_u[n]-\mathbf{w}_k\|^2$, constraints (26c) and (26d) are stricter than (22c) and (22d). Besides, problem (26) is equal to problem (22) when all the constraints in (26e) satisfy equality. Thus, the introduction of slack variables does not lose the optimality of problem (22).

We can find that constraints (26c)–(26e) are convex with respect to $S_k[n]$. But (25) and (26e) are not convex constraints for $\mathbf{w}_u[n]$, which make problem (26) still non-convex. Then we adopt the SCA to deal with the UAV trajectory.

The idea of SCA is to find a local solution (stationary point) of the original problem by iteratively solving a series of convex optimization problems approximate to the original problem. Since the first-order Taylor expansion of any convex function at any point is a global lower bound, and $R_k[n]$ in (25) is convex with respect to $\|\mathbf{w}_u[n]-\mathbf{w}_k\|^2$. Thus, $R_k[n]$ can be replaced by its first-order Taylor expansion while ensuring that the constraint (25) is still satisfied. Specifically, we define $\mathbf{W}^{r-1}$ as the optimized trajectory of the UAV in last iteration, and the first-order Taylor expansion lower-bound of $R_k[n]$ can be expressed as

$$\begin{aligned} R_k[n] &= B\log_2\left(1+\frac{P_k\rho_0}{\sigma^2\left(H^2+\|\mathbf{w}_u[n]-\mathbf{w}_k\|^2\right)}\right) \\ &\geq -C_k[n]\left(\|\mathbf{w}_u[n]-\mathbf{w}_k\|^2-\left\|\mathbf{w}_u^{r-1}[n]-\mathbf{w}_k\right\|^2\right) \\ &\quad + D_k[n], \end{aligned} \tag{27}$$

where $C_k[n]$ and $D_k[n]$ are constants calculated by

$$C_k[n] = \frac{\frac{BP_k\rho_0\log_2 e}{\left(H^2+\left\|\mathbf{w}_u^{r-1}[n]-\mathbf{w}_k\right\|^2\right)^2}}{\sigma^2+\frac{P_k\rho_0}{H^2+\left\|\mathbf{w}_u^{r-1}[n]-\mathbf{w}_k\right\|^2}}, \tag{28}$$

and

$$D_k[n] = B\log_2\left(1+\frac{P_k\rho_0}{\sigma^2\left(H^2+\|\mathbf{w}_u^{r-1}[n]-\mathbf{w}_k\|^2\right)}\right). \tag{29}$$

As for constraint (26e), because $\|\mathbf{w}_u[n]-\mathbf{w}_k\|^2$ is convex with respect to $\mathbf{w}_u[n]$, we perform the first-order Taylor expansion on it at $\mathbf{w}_u^{r-1}[n]$ and obtain its lower bound as following inequality

$$\|\mathbf{w}_u[n]-\mathbf{w}_k\|^2 \geq \left\|\mathbf{w}_u^{r-1}[n]-\mathbf{w}_k\right\|^2 + 2\left(\mathbf{w}_u^{r-1}[n]-\mathbf{w}_k\right)^T \times \left(\mathbf{w}_u[n]-\mathbf{w}_u^{r-1}[n]\right). \tag{30}$$

By substituting $R_k[n]$ in (25) and $\|\mathbf{w}_u[n]-\mathbf{w}_k\|^2$ in (26e) with (27) and (30) separately, we can approximate problem (26) as the following problem

$$\min_{\mathbf{W},\mathbf{S}} \sum_{n=1}^{N-1} E_{fly}[n] \tag{31}$$

$$\text{s.t. C1}: \ \mathbf{w}_u[1] = \mathbf{w}_u[N] \tag{31a}$$

$$\text{C2}: \ \|\mathbf{w}_u[n+1] - \mathbf{w}_u[n]\| \le V_{\max} t, \ n = 1, \ldots, N-1 \tag{31b}$$

$$\text{C3}: \ \sum_{k=1}^{K} I_k[n] B \log_2\left(1 + \frac{P_k \rho_0}{\sigma^2 (H^2 + S_k[n])}\right) t_{tr} \le \frac{(1 - r[n]) f_u[n]}{C} t_{\max}, \ \forall n \tag{31c}$$

$$\text{C4}: \ \sum_{k=1}^{K} I_k[n] B \log_2\left(1 + \frac{P_k \rho_0}{\sigma^2 (H^2 + S_k[n])}\right) t_{tr} \le \frac{R_u f_s}{r[n](f_s + R_u C)} t_{\max}, \ \forall n \tag{31d}$$

$$\text{C5}: \ S_k[n] \le \left\|\mathbf{w}_u^{r-1}[n] - \mathbf{w}_k\right\|^2 + 2\left(\mathbf{w}_u^{r-1}[n] - \mathbf{w}_k\right)^T \times \left(\mathbf{w}_u[n] - \mathbf{w}_u^{r-1}[n]\right), \ \forall k, n \tag{31e}$$

$$\text{C6}: \ \sum_{n=1}^{N} I_k[n] \left(-C_k[n] \left(\|\mathbf{w}_u[n] - \mathbf{w}_k\|^2 - \left\|\mathbf{w}_u^{r-1}[n] - \mathbf{w}_k\right\|^2\right) + D_k[n]\right) t_{tr} \ge L, \ \forall k. \tag{31f}$$

After approximation, (31e) is a linear constraint, and the left-hand-side of (31f) is concave for $\mathbf{w}_u[n]$, it is also a convex constraint with respect to $\mathbf{w}_u[n]$. Therefore, problem (31) is a convex optimization problem and can be efficiently solved by CVX.

C. Offloading and Resource Assignment

Based on the IoT devices' association strategies $\mathbf{I}$ solved in problem (20) and the UAV's trajectory $\mathbf{W}$ in problem (31), the offloading and resource assignment can be jointly optimized by the following problem

$$\min_{\mathbf{F},\mathbf{R}} \ \sum_{n=1}^{N} \left(E_{loc}[n] + E_{off}[n] + E_{rem}[n]\right) \tag{32}$$

$$\text{s.t. C1}: \ 0 \le f_u[n] \le F_u, \ \forall n \tag{32a}$$

$$\text{C2}: \ 0 \le f_s[n] \le F_s, \ \forall n \tag{32b}$$

$$\text{C3}: \ 0 \le r[n] \le 1, \ \forall n \tag{32c}$$

$$\text{C4}: \ \frac{(1 - r[n]) L[n] C}{f_u[n]} \le t_{\max}, \ \forall n \tag{32d}$$

$$\text{C5}: \ \frac{r[n] L[n]}{R_u} + \frac{r[n] L[n] C}{f_s[n]} \le t_{\max}, \ \forall n. \tag{32e}$$

The objective function is the total transmission and computation energy of the whole period, and the optimization variables are CPU frequencies allocation and offloading strategies in every time slot.

It is worth noting that in each time slot, optimization variables only affect the energy of this time slot and have no influence on the others, which means that the problem (32) can be divided into N independent subproblems. Thus, we reformulate problem (32) as

$$\min_{\mathbf{F},\mathbf{R}} \ E_{loc}[n] + E_{off}[n] + E_{rem}[n], \ \forall n \tag{33}$$

$$\text{s.t. (32a)–(32e)}. \tag{33a}$$

And the objective function of problem (33) can be expressed as the following function of variables $\mathbf{F}$ and $\mathbf{R}$

$$E_{loc}[n] + E_{off}[n] + E_{rem}[n] = L[n] \left(\psi f_u^2[n] (1 - r[n]) C + \frac{P_u r[n]}{R_u} + \varphi f_s^2[n] r[n] C\right). \tag{34}$$

To solve problem (33), we analyze the objective functions and constraints, and transform the problem. First, we have the following proposition.

Proposition 1: For the edge and central servers, ensuring the required CPU frequencies while increasing computation time $t_{loc}[n]$ and $t_{rem}[n]$ can reduce the computation energy consumption.

Proof: According to (8), we have the transformation $f_u[n] = \frac{(1 - r[n]) L[n] C}{t_{loc}[n]}$, i.e., the required CPU frequencies when the local computation time is specified as $t_{loc}[n]$. Further, we plug it into (9) and get

$$E_{loc}[n] = \psi \frac{(1 - r[n])^3 L^3[n] C^3}{t_{loc}^2[n]}, \tag{35}$$

which is a monotone decreasing function of $t_{loc}[n]$. The same is true for $E_{rem}[n]$ and $t_{rem}[n]$. So the proposition is proved.

Proposition 2: In the computation stage, to minimize computing energy consumption, i.e., $E_{loc}[n] + E_{rem}[n]$, the local computation time and the remote computation time need to be optimized to the upper limits so that $t_{loc}[n] = t_{off}[n] + t_{rem}[n] = t_{\max}$.

Proof: According to Proposition 1, the local and remote computing energy consumption can be reduced when we increase the computation time $t_{loc}[n]$ and $t_{off}[n]$. If $t_{loc}[n] \le t_{\max}$ or $t_{off}[n] + t_{rem}[n] \le t_{\max}$, we continue to add the smaller term until the two sides are equal, at which point the total energy consumption reaches the minimum in the current situation.

Then we can replace the local and remote computation time inequality constraints with equality constraints according to Proposition 2. And the problem can be transformed as

$$\min_{\mathbf{F},\mathbf{R}} \ E_{loc}[n] + E_{off}[n] + E_{rem}[n], \ \forall n \tag{36}$$

$$\text{s.t. C1}: \ \frac{(1 - r[n]) L[n] C}{f_u[n]} = t_{\max}, \ \forall n \tag{36a}$$

$$\text{C2}: \ \frac{r[n] L[n]}{R_u} + \frac{r[n] L[n] C}{f_s[n]} = t_{\max}, \ \forall n \tag{36b}$$

$$\text{C3}: \ \text{(32a)–(32c)}. \tag{36c}$$

Further, we can express computation frequencies $f_u[n]$ and $f_s[n]$ as the following functions of offloading strategies $r[n]$ by

transforming the constraints (36a) and (36b), i.e.,

$$f_u[n] = \frac{(1 - r[n]) L[n] C}{t_{\max}}, \tag{37}$$

and

$$f_s[n] = \frac{r[n] L[n] C}{t_{\max} - \frac{r[n]L[n]}{R_u}}. \tag{38}$$

Substituting (37) and (38) into (36) and reformulating the problem as

$$\min_{\mathbf{F},\mathbf{R}} \; E_{loc}[n] + E_{off}[n] + E_{rem}[n], \; \forall n \tag{39}$$

$$\text{s.t. C1}: \; 0 \le \frac{(1 - r[n]) L[n] C}{t_{\max}} \le F_u, \; \forall n \tag{39a}$$

$$\text{C2}: \; 0 \le \frac{r[n] L[n] C}{t_{\max} - \frac{r[n]L[n]}{R_u}} \le F_s, \; \forall n \tag{39b}$$

$$\text{C3}: \; 0 \le r[n] \le 1, \; \forall n, \tag{39c}$$

where constraints (36a) and (36b) are implict in (39a) and (39a) seperately. Now, the constraints involve only the variable $r[n]$, but the objective function still encompasses all variables. Hence, we need to transform the objective function. And it can be expressed as

$$\begin{aligned} &E_{loc}[n] + E_{off}[n] + E_{rem}[n] \\ &= \psi \frac{(1 - r[n])^2 L^2[n] C^2}{t_{\max}^2} (1 - r[n]) L[n] C \\ &\quad + \frac{P_u r[n] L[n]}{R_u} \\ &\quad + \varphi \frac{r^2[n] L^2[n] C^2}{(t_{\max} - \frac{r[n]L[n]}{R_u})^2} r[n] L[n] C \\ &= \frac{\psi (L[n] C)^3}{t_{\max}^2} (1 - r[n])^3 + \frac{P_u L[n]}{R_u} r[n] \\ &\quad + \varphi (L[n] C)^3 \frac{r^3[n]}{\left(t_{\max} - \frac{r[n]L[n]}{R_u}\right)^2}. \end{aligned} \tag{40}$$

After the transformation, the objective function includes only the variable $r[n]$, but its structure remains intricate. Then we derive the following proposition by analyzing the object function.

Proposition 3: The problem (39) is a convex optimization problem with respect to $r[n]$.

Proof: We can notice that (39a)–(39c) are linear constraints. Further, the first term of the objective function in (40) contains $(1 - r[n])^3$, which is a non-convex function but is convex with respect to $r[n]$ in the domain. As for the second term, it is linear with respect to $r[n]$. Denote the third term of the objective function with respect to $r[n]$ as f:

$$f = \frac{r^3[n]}{\left(t_{\max} - \frac{r[n]L[n]}{R_u}\right)^2}. \tag{41}$$

TABLE II
UNIVERSAL SIMULATION SPECIFICATIONS

Notation	Setting	Notation	Setting
K	8	σ^2	10^{-10} W
L	$32 * 10^6$ bits	R_u	$6 * 10^7$ bits/s
T	125 s	t_{tr}	0.5 s
H	30 m	C	1000 cycles/bit
N	25	ψ	10^{-26}
t	5 s	p_m	10 W
V_{max}	24 m/s	φ	10^{-26}
κ	1	t_{ex}	0.5 s
ρ_0	10^{-4}	F_u	$6*10^9$ cycles/s
B	10 MHz	F_s	$10*10^9$ cycles/s
P_k	1 W		

And the first derivative of f with respect to $r[n]$ can be presented as follows:

$$f' = \frac{3r^2[n]}{\left(t_{\max} - \frac{r[n]L[n]}{R_u}\right)^2} + \frac{2r^3[n] L[n]}{\left(t_{\max} - \frac{r[n]L[n]}{R_u}\right)^3 R_u}. \tag{42}$$

Further, the second derivative of f can be obtained as follows:

$$\begin{aligned} f'' = &\frac{6r[n]}{\left(t_{\max} - \frac{r[n]L[n]}{R_u}\right)^2} + \frac{6r^2[n] L[n]}{\left(t_{\max} - \frac{r[n]L[n]}{R_u}\right)^3 R_u} \\ &+ \frac{6r^2[n] L[n]}{\left(t_{\max} - \frac{r[n]L[n]}{R_u}\right)^3 R_u} + \frac{6r^3[n] L^2[n]}{\left(t_{\max} - \frac{r[n]L[n]}{R_u}\right)^4 R_u^2}. \end{aligned} \tag{43}$$

Because the offloading time is less than $t_{\max}$, so $t_{\max} - \frac{r[n]L[n]}{R_u}$ must be greater than zero. Then the second derivative of f is positive, i.e., f is convex with respect to $r[n]$. Thus, problem (39) is a convex optimization problem with respect to $r[n]$.

The convex problem (39) greatly simplifies the complexity compared to the original problem (32). Here we adopt the bisection-based method to search for the optimal value of $r[n]$. The main idea is to successively select intermediate values within the variable's defined domain, calculate and compare the objective function to determine the next selection. Specifically, initialize upper and lower bounds for $r[n]$, denoted as r_{upp} and r_{low}. Next, calculate their respective objective function values and compare them. Retain the boundary associated with the smaller value and set the value of the other boundary to $(r_{upp} + r_{low})/2$. The optimal value can be found with sufficient accuracy.

D. The Overall Algorithm

By iteratively solving the device association optimization, UAV's trajectory optimization, and offloading and resource assignment, we propose a Joint Association, Trajectory, Offloading and Resource (JATOR) optimization algorithm, as shown in Algorithm 1. Concretely, we first determine the UAV's trajectory and evenly offload tasks to edge and central servers for processing, while setting appropriate CPU frequencies to

Algorithm 1: JATOR Optimization Algorithm.

Input Initial variable sets $\mathbf{W}^0$, $\mathbf{F}_u^0$, $\mathbf{F}_s^0$, and $\mathbf{R}^0$.
for $r = 1 : \text{Max Iteration}$ **do**
  Based on $\mathbf{W}^{r-1}$, $\mathbf{F}_u^{r-1}$, $\mathbf{F}_s^{r-1}$, and $\mathbf{R}^{r-1}$, optimize the problem (20) to obtain the association strategies $\mathbf{I}^r$.
  Based on $\mathbf{I}^r$, $\mathbf{F}_u^{r-1}$, $\mathbf{F}_s^{r-1}$, and $\mathbf{R}^{r-1}$, optimize the problem (31) to obtain the trajectory of the UAV $\mathbf{W}^r$.
  for $n = 1 : N$ **do**
    Set r_{upp}, r_{low}, and the accuracy $\varepsilon = 0.01$.
    repeat
      Set $r[n] = (r_{upp} - r_{low})/2$.
      Calculate the object function (40) to get $f(r_{upp})$ and $f(r_{low})$.
      if $f(r_{upp}) \geq f(r_{low})$ **then**
        $r_{upp} = r[n]$.
      else
        $r_{low} = r[n]$.
        end if
    until $r_{upp} - r_{low} \leq \varepsilon$
  end for
  Obtain $\mathbf{R}^r$, and calculate $\mathbf{F}_u^r$ and $\mathbf{F}_s^r$ according to (37) and (38).
end for
Output Optimum sets $\mathbf{I}$, $\mathbf{W}$, $\mathbf{F}_u$, $\mathbf{F}_s$, and $\mathbf{R}$.

solve problem (20) and obtain the optimal solution for device association. Then, based on the obtained device association, we solve problem (31) to optimize the UAV's trajectory. Finally, using a bisection method, we iteratively solve for the optimal offloading ratio and calculate the optimal resource allocation based on the device association and UAV's trajectory. We repeat the above process until the final result converges (usually within ten iterations).

V. Experiment Results and Analysis

We conduct a significant number of simulations to comprehensively demonstrate the performance of the designed architecture and proposed algorithms. The simulation specifications are presented in detail in Table II. The specific values of other variables are illustrated in charts and explained in the simulation. To evaluate the effectiveness of the designed JATOR scheme, we compare it with three other schemes as follows. The comparison is carried out by analyzing various performance metrics, allowing us to assess the strengths of the proposed scheme in comparison to the other three.

- *Remote Computation scheme:* This scheme is based on the network architecture proposed in [16], [19], [20], [21], where only base stations act as servers to process tasks from devices. In this scheme, the device association and the UAV's trajectory are iteratively optimized, and all the data is offloaded to the TBS.
- *Local Computation scheme:* This scheme is based on the UAV-centric MEC networks proposed in [24], [25], [28], [29], where UAVs fly over the area to process tasks from devices. It simultaneously optimizes the association strategies of IoT devices and the flight trajectory of UAVs, with all offloading data restricted to local computation on the UAV.
- *Circular Trajectory scheme:* This scheme refers to the circular trajectory approach described in [38]. It collectively optimizes association strategies, offloading, and resource assignment using the proposed algorithm, while the UAV hovers in a circular trajectory above the area. We adopt this scheme to demonstrate the effect of UAV's trajectory optimization.

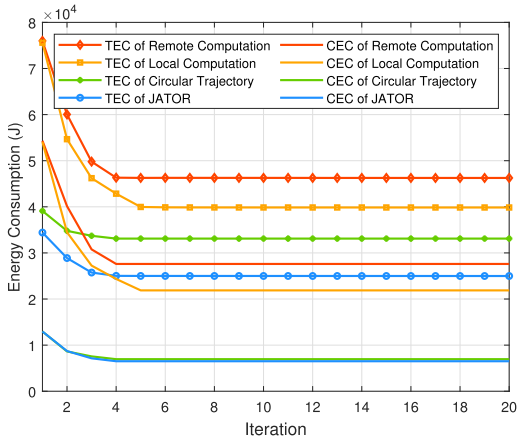

Fig. 4. Total and computing energy consumption trends with iteration.

To assess the convergence of the proposed algorithms, we conduct simulations on the total energy consumption (TEC) and computing energy consumption (CEC) of the four schemes, tracking their performance with respect to the number of iterations. As shown in Fig. 4, the convergence curves of each scheme indicate a stable pattern as the number of iterations increases. The results obtained from the first iteration are significantly higher than those of the subsequent results, since we set the initial values of the simulation broadly to ensure an feasible solution under various parameters. Furthermore, in the subsequent iterations, the reduction in energy consumption becomes smaller, converging at around five iterations. Hence, it can be deduced that the proposed algorithms demonstrate rapid convergence speed.

Fig. 5 illustrates a simulated scenario in which the TBS is located at the origin and represented by the yellow triangle. The IoT devices are non-uniformly distributed in the area and represented by green crosses, positioned at (250, 0), (400, 400), (100, 300), (−250, 250), (−400, 0), (−300, −300), (0, −400), and (400, −300) [2]. The red, orange, and blue dashed lines and dots in the figure respectively represent the optimal flight trajectory and discrete locations of the UAV when the total number of time slots is 15, 25, and 35 (the amount of data L also changes proportionally). It is apparent that with an increase in the total number of time slots, the flight range of the UAV expands and the distance to the IoT devices decreases, demonstrating a certain correlation between the trajectory and the distribution of the IoT devices. Based on the optimized UAV's trajectories,

[2]In this paper, we employ small rotary-wing UAV with limited computing capability, serving a relatively small number of users. Hence, the number of devices in the simulation is intentionally kept low. Similar parameters settings have been widely employed in other related works [24], [26], [27], [28], [29].

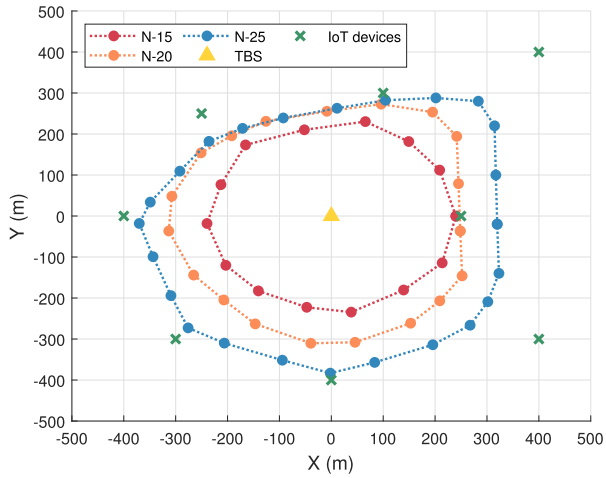

Fig. 5. Scenario and trajectories of the UAV with different loads.

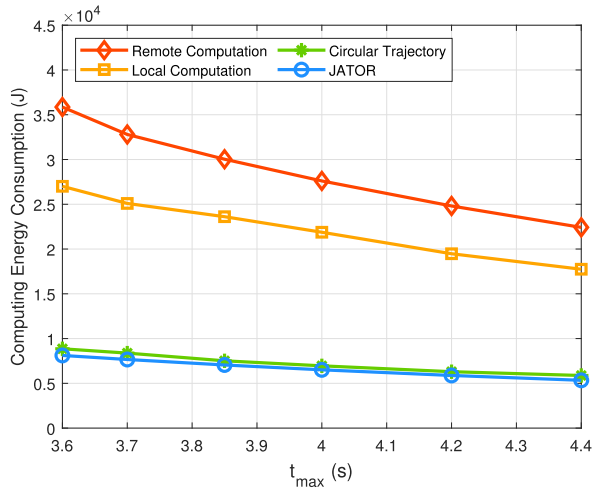

Fig. 7. Effect of the maximal length of computation stage $t_{\max}$ on computing energy consumption.

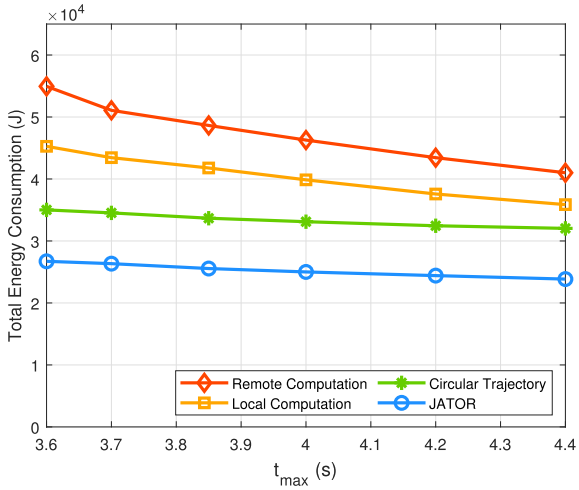

Fig. 6. Effect of the maximal length of computation stage $t_{\max}$ on total energy consumption.

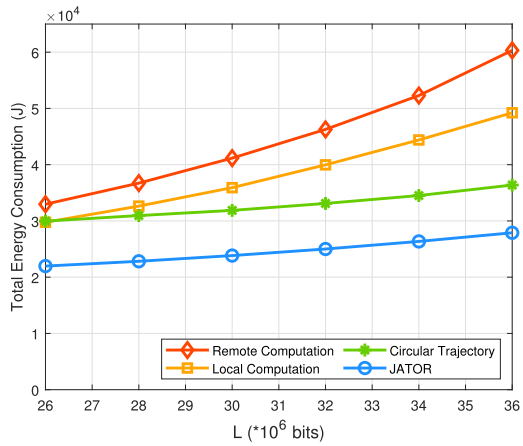

Fig. 8. Effect of the amount of data L on total energy consumption.

it can be observed that the UAV tends to approach the TBS to minimize flight energy consumption when the network load is low. However, when the load is high, the UAV must approach the IoT devices to collect data. This is because although the flight energy consumption of the UAV accounts for a large proportion of the objective function, the trend of reducing the UAV's trajectory is also constrained by data transmission, and the two factors ultimately reach a balance with the progress of iterations.

Fig. 6 shows the impact of the maximal length of computing stage $t_{\max}$ on the TEC for four different schemes. From the figure, it can be seen that the TEC of the Remote Computation scheme is always the highest, followed by the Local Computation scheme and the Circular Trajectory scheme, while the JATOR scheme has the best performance among the four schemes. Furthermore, with an increase in $t_{\max}$, all four schemes display a decreasing trend in TEC. Additionally, the difference between the Local Computation scheme and the Circular Trajectory scheme diminishes as $t_{\max}$ increases.

To further investigate the impact of the maximal length of the computation stage, we analyze the variations in CEC for the schemes, as illustrated in Fig. 7. All four schemes exhibit a noticeable decline in CEC with an increase in $t_{\max}$, which is consistent with the trend observed in Fig. 6. Moreover, $t_{\max}$ has a more significant impact on CEC. According to Proposition 1, extending the computation stage results in a reduction of computing energy consumption, which explains the observed trend in the figure. It is worth noting that the Circular Trajectory scheme only has slightly higher CEC compared to the JATOR scheme, and the two are very similar. This is because the Circular Trajectory scheme simultaneously optimizes access control and offload and resource assignment, the performance loss caused by the deficiency of the trajectory is relatively small in terms of computing energy consumption. In addition, it can be observed that there is a clear trade-off between $t_{\max}$ and the CEC. Therefore, when designing the network, tasks with different latency requirements need to be reasonably partitioned.

Fig. 8 illustrates the influence of the amount of data generated by IoT devices on TEC. As shown in the figure, the TEC of the

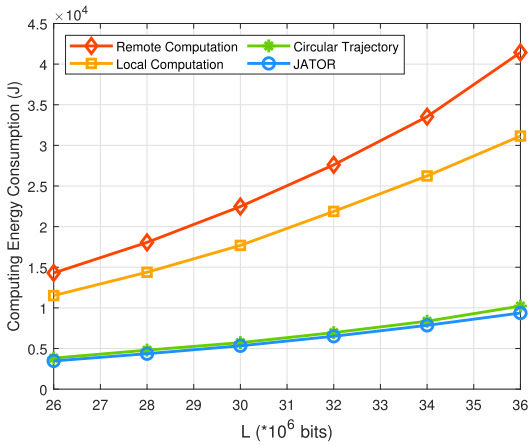

Fig. 9. Effect of the amount of data L on computing energy consumption.

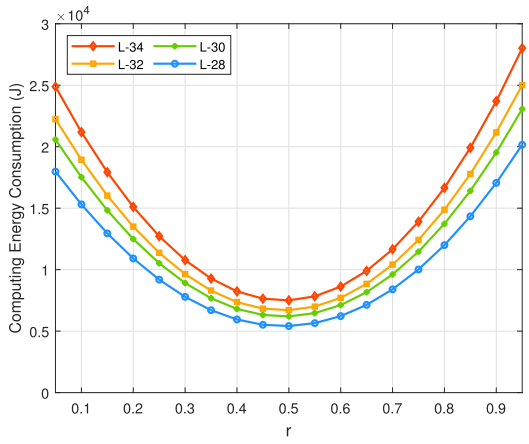

Fig. 10. Computing energy consumption trends with varying offloading ratios.

four schemes increases non-linearly with the increase of L, and the Remote Computing scheme experiences the most significant rise. When L is relatively small (i.e., $L = 26 * 10^6$), the TEC of the Local Computing and Circular Trajectory schemes are comparable. However, the performance of the Local Computing scheme deteriorates rapidly as L increases, indicating the limitations of unreasonable task offloading. The TEC of the Circular Trajectory and JATOR schemes is relatively less affected by the changes in L, and the stable difference between the two is maintained.

Fig. 9 shows the trend of CEC for four different schemes as the amount of data L varies. It is noticeable that compared to TEC, CEC exhibits a more pronounced change. By analyzing the difference between the two, it can be inferred that the energy consumption, except for CEC (mainly flight energy E_{fly}), does not change much, which implies that L has a more direct influence on CEC. According to formula (21), the relationship between CEC and L follows a quadratic growth, which is also well demonstrated by the simulated changes shown in Fig. 9. Further, the Circular Trajectory scheme incurs slightly higher CEC than the JATOR scheme as with Fig. 7. Unlike the exponential growth trend observed in the Remote and Local Computation schemes, both exhibit a relatively stable growth trend. It is worth noting that although the CEC of the Circular Trajectory scheme is much smaller than that of the Local Computation scheme when $L = 26 * 10^6$, their TECs are comparable. This indicates that the flight energy of the Circular Trajectory scheme is quite large, underscoring the importance of considering energy gain brought by UAV's trajectory optimization.

In addition to $t_{\max}$ and L, we analyze the CEC of objective function with different L ($\{28, 30, 32, 34\} * 10^6$) under various offloading ratios r, as depicted in Fig. 10. It is observed that the CEC for all four schemes initially decreases and then increases as r increases, with the optimal CEC value corresponding to r around 0.5. When r approaches 0 or 1, the CEC rises sharply (corresponding to the CEC of Local and Remote Computation schemes under the same parameters). Furthermore, as Proposition 3 proves, the CEC is a convex function of r, and the changing curves provide good validation. Finally, the curves are not perfectly symmetrical about 0.5, and the optimal offloading ratio is highly dependent on network parameter settings. Various factors such as effective capacitance of server, amount of data, and other conditions will affect the optimal value as stated in formula (40). To be more specific, for servers with smaller effective capacitance coefficient ψ or φ, performing computations is beneficial for energy conservation. When the data amount is high, local computation is preferred to reduce CEC. Additionally, a higher communication rate R_u contributes to lowering CEC.

VI. Conclusion

We have designed a novel dynamic UAV-assisted MEC system with optimizations for device association, UAV-trajectroy planning, task offloading, and resource assignment in order to minimize the total energy consumption. To solve the problem, we have adopted the BCD and SCA methods to separate the problem into three sub-problems. We have transformed them into tractable linear programming or convex problems, and proposed the JATOR algorithm to iteratively solve these sub-problems. In addition, we have derived the optimal relationship between computation duration and computing energy, which greatly reduces the complexity of the problems. And we have found that various factors such as server parameters, amount of data, and communication rate affect the optimal offloading ratio. Simulation results have shown that the proposed network and algorithm effectively reduce the total energy consumption, demonstrating the efficacy of our approach.

In our future work, we will consider introducing more UAVs in MEC networks and addressing interference among users under various UAV coverage scenarios. The collaborative relationships among UAVs will increase the complexity of joint optimization problems. Furthermore, the introduction of interference will bring new challenges, such as channel allocation. Building upon the current work, we will further explore the joint optimization of air-ground collaborative MEC networks.

REFERENCES

[1] K. Shafique, B. A. Khawaja, F. Sabir, S. Qazi, and M. Mustaqim, "Internet of Things (IoT) for next-generation smart systems: A review of current challenges, future trends and prospects for emerging 5G-IoT scenarios," *IEEE Access*, vol. 8, pp. 23022–23040, 2020.

[2] J. Feng, L. Liu, X. Hou, Q. Pei, and C. Wu, "QoE fairness resource allocation in digital twin-enabled wireless virtual reality systems," *IEEE J. Sel. Areas Commun.*, vol. 41, no. 11, pp. 3355–3368, Nov. 2023.

[3] X. Shen, J. Gao, W. Wu, M. Li, C. Zhou, and W. Zhuang, "Holistic network virtualization and pervasive network intelligence for 6G," *IEEE Commun. Surv. Tuts.*, vol. 24, no. 1, pp. 1–30, Firstquarter 2022.

[4] M. Vaezi et al., "Cellular, wide-area, and non-terrestrial IoT: A survey on 5G advances and the road toward 6G," *IEEE Commun. Surv. Tuts.*, vol. 24, no. 2, pp. 1117–1174, Secondquarter 2022.

[5] L. Chettri and R. Bera, "A comprehensive survey on Internet of Things (IoT) toward 5G wireless systems," *IEEE Internet Things J.*, vol. 7, no. 1, pp. 16–32, Jan. 2020.

[6] D. Zhai, C. Wang, R. Zhang, H. Cao, and F. R. Yu, "Energy-saving deployment optimization and resource management for UAV-assisted wireless sensor networks with NOMA," *IEEE Trans. Veh. Technol.*, vol. 71, no. 6, pp. 6609–6623, Jun. 2022.

[7] F. Spinelli and V. Mancuso, "Toward enabled industrial verticals in 5G: A survey on MEC-based approaches to provisioning and flexibility," *IEEE Commun. Surv. Tuts.*, vol. 23, no. 1, pp. 596–630, Firstquarter 2021.

[8] Y. Siriwardhana, P. Porambage, M. Liyanage, and M. Ylianttila, "A survey on mobile augmented reality with 5G mobile edge computing: Architectures, applications, and technical aspects," *IEEE Commun. Surv. Tuts.*, vol. 23, no. 2, pp. 1160–1192, Secondquarter 2021.

[9] P. Porambage, J. Okwuibe, M. Liyanage, M. Ylianttila, and T. Taleb, "Survey on multi-access edge computing for Internet of Things realization," *IEEE Commun. Surv. Tuts.*, vol. 20, no. 4, pp. 2961–2991, Fourthquarter 2018.

[10] L. Liu, J. Feng, X. Mu, Q. Pei, D. Lan, and M. Xiao, "Asynchronous deep reinforcement learning for collaborative task computing and on-demand resource allocation in vehicular edge computing," *IEEE Trans. Intell. Transp. Syst.*, vol. 24, no. 12, pp. 15513–15526, Dec. 2023.

[11] C. Wang, D. Zhai, H. Cao, R. Zhang, and H. Li, "Dynamic UAV deployment, admission control, and power control for air-and-ground cooperative networks," in *Proc. IEEE Int. Conf. Commun.*, 2022, pp. 1–6.

[12] M. M. Azari et al., "Evolution of non-terrestrial networks from 5G to 6G: A survey," *IEEE Commun. Surv. Tuts.*, vol. 24, no. 4, pp. 2633–2672, Fourthquarter 2022.

[13] Y. He, F. Huang, D. Wang, R. Zhang, X. Gu, and J. Pan, "NOMA- and MRC-enabled framework in drone-relayed vehicular networks: Height/trajectory optimization and performance analysis," *IEEE Internet Things J.*, vol. 10, no. 24, pp. 22305–22319, Dec. 2023.

[14] M. Abrar, U. Ajmal, Z. M. Almohaimeed, X. Gui, R. Akram, and R. Masroor, "Energy efficient UAV-enabled mobile edge computing for IoT devices: A review," *IEEE Access*, vol. 9, pp. 127779–127798, 2021.

[15] Y. He, D. Wang, F. Huang, R. Zhang, X. Gu, and J. Pan, "A V2I and V2V collaboration framework to support emergency communications in ABS-aided Internet of Vehicles," *IEEE Trans. Green Commun. Netw.*, vol. 7, no. 4, pp. 2038–2051, Dec. 2023.

[16] Z. Ding, D. Xu, R. Schober, and H. V. Poor, "Hybrid NOMA offloading in multi-user MEC networks," *IEEE Trans. Wireless Commun.*, vol. 21, no. 7, pp. 5377–5391, Jul. 2022.

[17] Y. Ye, L. Shi, H. Sun, R. Q. Hu, and G. Lu, "System-centric computation energy efficiency for distributed NOMA-based MEC networks," *IEEE Trans. Veh. Technol.*, vol. 69, no. 8, pp. 8938–8948, Aug. 2020.

[18] M. Guo, W. Wang, X. Huang, Y. Chen, L. Zhang, and L. Chen, "Lyapunov-based partial computation offloading for multiple mobile devices enabled by harvested energy in MEC," *IEEE Internet Things J.*, vol. 9, no. 11, pp. 9025–9035, Jun. 2022.

[19] Y. Ye, L. Shi, X. Chu, R. Q. Hu, and G. Lu, "Resource allocation in backscatter-assisted wireless powered MEC networks with limited MEC computation capacity," *IEEE Trans. Wireless Commun.*, vol. 21, no. 12, pp. 10678–10694, Dec. 2022.

[20] H. Hu, W. Song, Q. Wang, R. Q. Hu, and H. Zhu, "Energy efficiency and delay tradeoff in an MEC-enabled mobile IoT network," *IEEE Internet Things J.*, vol. 9, no. 17, pp. 15942–15956, Sep. 2022.

[21] B. Liu, C. Liu, and M. Peng, "Resource allocation for energy-efficient MEC in NOMA-enabled massive IoT networks," *IEEE J. Sel. Areas Commun.*, vol. 39, no. 4, pp. 1015–1027, Apr. 2021.

[22] R. Malik and M. Vu, "Energy-efficient joint wireless charging and computation offloading in MEC systems," *IEEE J. Sel. Topics Signal Process.*, vol. 15, no. 5, pp. 1110–1126, Aug. 2021.

[23] W. Zhang, G. Zhang, and S. Mao, "Joint parallel offloading and load balancing for cooperative-MEC systems with delay constraints," *IEEE Trans. Veh. Technol.*, vol. 71, no. 4, pp. 4249–4263, Apr. 2022.

[24] Z. Yang, S. Bi, and Y.-J. A. Zhang, "Online trajectory and resource optimization for stochastic UAV-enabled MEC systems," *IEEE Trans. Wireless Commun.*, vol. 21, no. 7, pp. 5629–5643, Jul. 2022.

[25] J. Ji, K. Zhu, C. Yi, and D. Niyato, "Energy consumption minimization in UAV-assisted mobile-edge computing systems: Joint resource allocation and trajectory design," *IEEE Internet Things J.*, vol. 8, no. 10, pp. 8570–8584, May 2021.

[26] M. Li, N. Cheng, J. Gao, Y. Wang, L. Zhao, and X. Shen, "Energy-efficient UAV-assisted mobile edge computing: Resource allocation and trajectory optimization," *IEEE Trans. Veh. Technol.*, vol. 69, no. 3, pp. 3424–3438, Mar. 2020.

[27] X. Zhang, J. Zhang, J. Xiong, L. Zhou, and J. Wei, "Energy-efficient multi-UAV-enabled multiaccess edge computing incorporating NOMA," *IEEE Internet Things J.*, vol. 7, no. 6, pp. 5613–5627, Jun. 2020.

[28] Z. Yang, S. Bi, and Y.-J. A. Zhang, "Dynamic offloading and trajectory control for UAV-enabled mobile edge computing system with energy harvesting devices," *IEEE Trans. Wireless Commun.*, vol. 21, no. 12, pp. 10515–10528, Dec. 2022.

[29] C. Zhan, H. Hu, X. Sui, Z. Liu, and D. Niyato, "Completion time and energy optimization in the UAV-enabled mobile-edge computing system," *IEEE Internet Things J.*, vol. 7, no. 8, pp. 7808–7822, Aug. 2020.

[30] X. Duan, Y. Zhou, D. Tian, J. Zhou, Z. Sheng, and X. Shen, "Weighted energy-efficiency maximization for a UAV-assisted multiplatoon mobile-edge computing system," *IEEE Internet Things J.*, vol. 9, no. 19, pp. 18208–18220, Oct. 2022.

[31] T. Zhang, Y. Xu, J. Loo, D. Yang, and L. Xiao, "Joint computation and communication design for UAV-assisted mobile edge computing in IoT," *IEEE Trans. Ind. Informat.*, vol. 16, no. 8, pp. 5505–5516, Aug. 2020.

[32] Y. Liu, K. Xiong, Q. Ni, P. Fan, and K. B. Letaief, "UAV-assisted wireless powered cooperative mobile edge computing: Joint offloading, CPU control, and trajectory optimization," *IEEE Internet Things J.*, vol. 7, no. 4, pp. 2777–2790, Apr. 2020.

[33] C. Zhou et al., "Deep reinforcement learning for delay-oriented IoT task scheduling in SAGIN," *IEEE Trans. Wireless Commun.*, vol. 20, no. 2, pp. 911–925, Feb. 2021.

[34] Q. Wu, Y. Zeng, and R. Zhang, "Joint trajectory and communication design for multi-UAV enabled wireless networks," *IEEE Trans. Wireless Commun.*, vol. 17, no. 3, pp. 2109–2121, Mar. 2018.

[35] Y. Zeng, J. Xu, and R. Zhang, "Energy minimization for wireless communication with rotary-wing UAV," *IEEE Trans. Wireless Commun.*, vol. 18, no. 4, pp. 2329–2345, Apr. 2019.

[36] B. Liu, Y. Wan, F. Zhou, Q. Wu, and R. Q. Hu, "Resource allocation and trajectory design for MISO UAV-assisted MEC networks," *IEEE Trans. Veh. Technol.*, vol. 71, no. 5, pp. 4933–4948, May 2022.

[37] X. Hu, K.-K. Wong, K. Yang, and Z. Zheng, "UAV-assisted relaying and edge computing: Scheduling and trajectory optimization," *IEEE Trans. Wireless Commun.*, vol. 18, no. 10, pp. 4738–4752, Oct. 2019.

[38] X. Diao, W. Yang, L. Yang, and Y. Cai, "UAV-relaying-assisted multi-access edge computing with multi-antenna base station: Offloading and scheduling optimization," *IEEE Trans. Veh. Technol.*, vol. 70, no. 9, pp. 9495–9509, Sep. 2021.

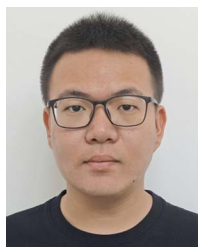

Chen Wang received the B.E. degree in telecommunication engineering, in 2020 from Northwestern Polytechnical University, Xi'an, China, where he is currently working toward the Ph.D. degree in communication and information systems. His research focuses on resource management in air-ground cooperative edge computing networks.

Daosen Zhai (Member, IEEE) received the B.E. degree in telecommunication engineering from Shandong University, Weihai, China, in 2012, and the Ph.D. degree in communication and information systems from Xidian University, Xi'an, China, in 2017. He is currently an Associate Professor with the School of Electronics and Information, Northwestern Polytechnical University, Xi'an. His research interests include B5G and 6G key techniques, massive access techniques, air-and-ground integrated network, and convex optimization, and graph theory and their applications in wireless communications.

Ruonan Zhang (Member, IEEE) received the B.S. and M.Sc. degrees in electrical and electronics engineering from Xi'an Jiaotong University, Xi'an, China, in 2000 and 2003, respectively, and the Ph.D. degree in electrical and electronics engineering from the University of Victoria, Victoria, BC, Canada, in 2010. He was an IC Design Engineer with Motorola Inc. and Freescale Semiconductor Inc., Tianjin, China, from 2003 to 2006. Since 2010, he has been with the Department of Communication Engineering, Northwestern Polytechnical University, Xi'an, where he is currently a Professor. His research interests include wireless channel measurement and modeling, architecture and protocol design of wireless networks, and satellite communications. He was a Local Arrangement Co-Chair for the IEEE/CIC International Conference on Communications in China (ICCC) in 2013, Industry Track and Workshop Chair for the IEEE International Conference on High Performance Switching and Routing (HPSR) in 2019, and an Associate Editor for the *Journal of Communications and Networks*. He was the recipient of the New Century Excellent Talent Grant from the Ministry of Education of China.

Lin Cai (Fellow, IEEE) has been with the Department of Electrical & Computer Engineering at the University of Victoria since 2005 and is currently a Professor. Her research interests include several areas in communications and networking, with a focus on network protocol and architecture design supporting ubiquitous intelligence. She is an NSERC E.W.R. Steacie Memorial Fellow, a Canadian Academy of Engineering (CAE) Fellow, and an Engineering Institute of Canada (EIC) Fellow. In 2020, she was elected as a Member of the Royal Society of Canada's College of New Scholars, Artists and Scientists, and a 2020 "Star in Computer Networking and Communications" by N2Women. She co-founded and chaired the IEEE Victoria Section Vehicular Technology and Communications Joint Societies Chapter. She has elected to serve the IEEE Vehicular Technology Society (VTS) Board of Governors, during 2019–2024, and was its VP Mobile Radio from 2023 to 2024. She was a Board Member of IEEE Women in Engineering from 2022 to 2024, and a Board Member of IEEE Communications Society (ComSoc) from 2024 to 2026. She has held various editorial roles, including Associate Editor-in-Chief for IEEE TRANSACTIONS ON VEHICULAR TECHNOLOGY and membership in the Steering Committee of IEEE TRANSACTIONS ON MOBILE COMPUTING, IEEE TRANSACTIONS ON BIG DATA, and IEEE TRANSACTIONS ON CLOUD COMPUTING. She has also been an Associate Editor for IEEE/ACM TRANSACTIONS ON NETWORKING, IEEE INTERNET OF THINGS JOURNAL, IEEE TRANSACTIONS ON WIRELESS COMMUNICATIONS, IEEE TRANSACTIONS ON VEHICULAR TECHNOLOGY, AND IEEE TRANSACTIONS ON COMMUNICATIONS. Lin Cai is a Distinguished Lecturer of the IEEE VTS and IEEE Communications Societies, and a registered Professional Engineer in British Columbia, Canada. She was the recipient of the NSERC Discovery Accelerator Supplement (DAS) Grants in 2010 and 2015, respectively.

Lei Liu (Member, IEEE) received the B.Eng. degree in electronic information engineering from Zhengzhou University, Zhengzhou, China, in 2010, and the M.Sc. and Ph.D. degrees in communication and information systems from Xidian University, Xian, China, in 2013 and 2019, respectively. From 2013 to 2015, he was with a subsidiary of China Electronics Corporation. From 2018 to 2019, he was supported by China Scholarship Council to be a visiting Ph.D. student with the University of Oslo, Oslo, Norway. He is currently an Associate Professor with the Guangzhou Institute of Technology, Xidian University. His research interests include vehicular ad hoc networks, intelligent transportation, mobile-edge computing, and Internet of Things.

Mianxiong Dong (Member, IEEE) received the B.S., M.S. and Ph.D. degrees in computer science and engineering from The University of Aizu, Aizuwakamatsu, Japan, in 2006, 2008, and 2013, respectively. He was a JSPS Research Fellow with the School of Computer Science and Engineering, The University of Aizu, and was a Visiting Scholar with BBCR group, University of Waterloo, Waterloo, ON, Canada, supported by JSPS Excellent Young Researcher Overseas Visit Program from 2010 to 2011. He is currently the Vice President and a Professor with the Muroran Institute of Technology, Muroran, Japan. Dr. Dong was selected as a Foreigner Research Fellow (a total of 3 recipients all over Japan) by NEC C&C Foundation in 2011. He is Clarivate Analytics 2019, 2021, 2022, and 2023 Highly Cited Researcher (Web of Science) and Foreign Fellow of EAJ. He was the recipient of the 12th IEEE ComSoc Asia-Pacific Young Researcher Award 2017, Funai Research Award 2018, NISTEP Researcher 2018 (one of only 11 people in Japan) in recognition of significant contributions in science and technology, Young Scientists' Award from MEXT in 2021, SUEMATSU-Yasuharu Award from IEICE in 2021, IEEE TCSC Middle Career Award in 2021.